Catal Lett (2009) 130:239–245
DOI 10.1007/s10562-009-9875-4

Development of a Catalytic Cycle in Molybdenum Carbide Catalyzed NO/CO Reaction

Zhiwei Yao · Chuan Shi

Received: 2 December 2008 / Accepted: 21 January 2009 / Published online: 5 February 2009

Abstract In NO/CO reaction, there is a competition between NO reduction by CO and Mo_2C oxidation by oxygen generated during NO dissociation. A complete equality of NO conversion and NO reduction degree can be achieved after increasing CO concentration in the system, which makes establishing a catalytic cycle on Mo_2C catalyst possible.

Keywords Mo_2C · NO reduction · NO dissociation · Catalytic cycle

1 Introduction

Air pollution induced by nitrogen oxides (NO_x) in the exhaust gases from automobiles and power plants has become a serious problem. Therefore, the development of excellent catalysts to remove NO_x is of great importance. Several different catalytic systems such as ion exchanged zeolite [1–3], noble metals [4–6] and metal oxide catalysts [7–9] have been investigated for the dissociation of NO in the absence/presence of reducing agents. Catalytic dissociation of NO to N_2 is the best way for NO removal. However, most of catalysts are more active for NO dissociation to N_2 in the higher reaction temperature region and just the supported noble metal catalyst system [10–12] is active in the lower temperature region.

Due to the catalytic properties being similar to those of noble metals, molybdenum carbides have attracted much attention in heterogeneous catalysis. For example, these materials show good catalytic activities in carbon monoxide hydrogenation [13], ammonia synthesis [14], and methane reforming [15, 16] as well as in hydrodesulfurization (HDS) and hydrodenitrogenation (HDN) reactions [17–19]. It has been reported that low-temperature N_2O and N_2 desorption features were observed in NO-TPD study of Mo_2C [20]. Zhang et al. [21] also reported the decomposition of NO on carbide-modified Mo surfaces, where Mo was epitaxially grown on the W (111) substrate through physical vapor deposition. Based on these characteristics of molybdenum carbide, it was envisaged that the material could be a good catalyst for the direct decomposition of NO. Recently, Ji et al. [22] conducted investigations on NO decomposition over molybdenum carbide catalysts. It was found that high NO decomposition activity on bulk Mo_2C and Mo_2C/γ-Al_2O_3 catalysts was similar to that on noble metal based catalysts. However, many details were still missing about the possible formation of oxygen phase in NO decomposition reaction, and the reaction pathways were envisaged to perfect.

In this study, we focus on the exploration of Mo_2C for NO reduction with CO. Techniques of X-ray diffraction (XRD), temperature-programmed decomposition (TPD), temperature-programmed oxidation (TPO), O_2-uptake and temperature-programmed-reaction (TPR) were adopted for the structural characterization of the catalyst, and to give insights into the catalytic nature of Mo_2C for NO reduction with CO. Simultaneously, a possible route for keeping the catalyst stable and active was proposed.

Z. Yao · C. Shi (✉)
Laboratory of Plasma Physical Chemistry, Dalian University of Technology, 116024 Dalian, People's Republic of China
e-mail: chuanshi@dlut.edu.cn

Z. Yao
e-mail: mezhiwei@163.com

C. Shi
State Key Laboratory of Fine chemicals, Dalian University of Technology, 116024 Dalian, People's Republic of China

2 Experimental

2.1 Catalyst Preparation

Molybdenum carbide, Mo_2C, was prepared according to the CH_4/H_2-temperature-programmed reduction procedure described by Thompson and co-workers [23]. Typically, about 2.0 g of the MoO_3 precursor was placed in a micro-reactor and a flow of 20% CH_4/H_2 (150 ml/min) was introduced into the system. The temperature was increased from room temperature (RT) to 300 °C over a period of 30 min followed by a rise in temperature from 300 to 700 °C at a rate of 1 °C/min. The temperature was then kept at 700 °C for 2 h before quenching to RT in a 20%CH_4/H_2 flow. Finally, the material was passivated in 1%O_2/He for 12 h before it was exposed to air.

2.2 Catalyst Characterization

XRD examination was performed using a X-ray diffractometer (Rigaku D-Max Rotaflex) with Cu $K\alpha$ radiation ($\lambda = 1.5404$ Å) in the 2θ range from 20 to 90° at a step size of 0.06°.

TPD experiment was carried out with a fixed-bed quartz reactor. one hundred and fifty milligram of sample was directly heated in flowing He (50 ml/min) at a rate of 15 °C/min to 750, 850 and 950 °C, respectively, followed by cooling to RT under He flow, and then passivated at RT in a stream of 1%O_2/He for 2 h.

TPO experiment was tested on a flow system equipped with a mass spectrometer (MS, HP G1800A). The sample (25 mg) was submitted to a heat treatment in He flow at 500 °C for 1 h. After being cooled to RT, the sample was directly heated to 700 °C at a heating rate of 15 °C/min under a flow of 10%O_2/He (50 ml/min). The signal of $m/e = 32$ was continuously detected by MS.

The O_2-uptake experiments were measured by injecting a standard volume (101 μl) of pure O_2 via a calibrated sample loop at 5 min intervals into the sample using He as carrier gas until there was no detectable oxygen uptake. Prior to adsorption, the sample was pretreated in He at 500 °C for 1 h.

TPR experiment was performed on a flow reaction system. The catalyst (400 mg) was pretreated in He flow at 500 °C for 1 h, and then cooled to 200 °C. After thermal stability was reached, the temperature was raised to 600 °C at 15 °C/min in 0.3%NO/He (50 ml/min). The effluent gases were continuously monitored with a mass spectrometer (MS, HP G1800A) for the analysis of $m/e = 30$ (NO), $m/e = 32$ (O_2), $m/e = 28$ (N_2 or CO) and $m/e = 44$ (N_2O or CO_2), and an infrared absorption spectrometer (IRAS, SICK-MAIHAK-S710) for that of N_2O, CO and CO_2.

2.3 Catalyst Activity

The catalytic activity was measured using a micro-catalytic reactor by feeding a gas mixture of 0.1%NO/0.1–0.3%CO/He for the reduction studies. Typically, the catalyst (400 mg) was pretreated in pure He at 400 °C for 1 h before the reaction. At a flow rate of 20 cm^3 min^{-1}, the corresponding W/F was 1.2 $gscm^{-3}$. The effluent gases were monitored by online GC using a molecular sieve 5A column (3 m, ϕ4) with a thermal conductivity detector (for the analysis of O_2, N_2, CO and NO), as well as a mass spectrometer (MS, HP G1800A) and an infrared absorption spectrometer (IRAS, SICK-MAIHAK-S710) (for that of CO_2, N_2O and other possible nitrogen oxides).

3 Results and Discussion

3.1 Structural Properties

XRD pattern of the as-prepared Mo_2C sample is shown in Fig. 1. The lines at 34.5°, 38.0°, 39.5°, 52.2°, 61.6°,69.6°, 74.6° and 75.6° corresponded to the {002}, {200}, {102}, {202}, {023}, {302}, {223} and {142} reflections of β-Mo_2C, respectively. There were no lines that can be assigned to molybdenum oxide(s) or other carbides, indicating that the Mo_2C material was phase-pure.

To investigate the structural stability of Mo_2C sample in an inert atmosphere, we heated the sample to 750, 850 and 950 °C, respectively, in a flow of He. Figure 2 shows the changes in the XRD patterns of the Mo_2C sample during the heating treatment in He. On heating Mo_2C sample

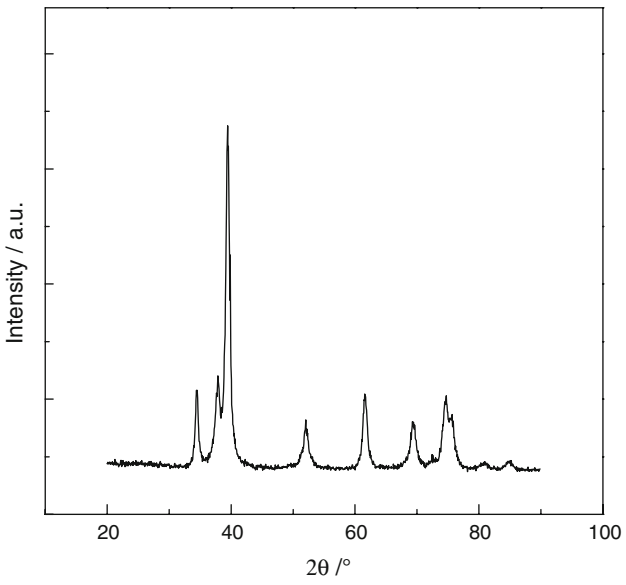

Fig. 1 XRD pattern of as-prepared Mo_2C sample

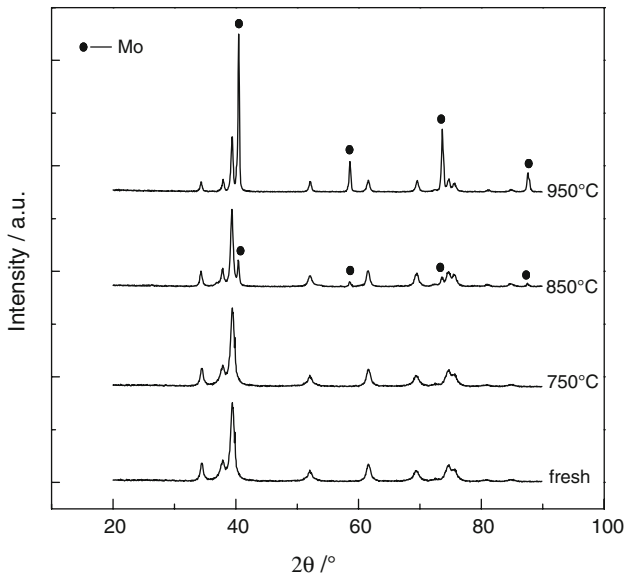

Fig. 2 XRD patterns of the Mo_2C sample during the heating treatment in He at different temperatures. The pattern of fresh Mo_2C is also shown for comparison

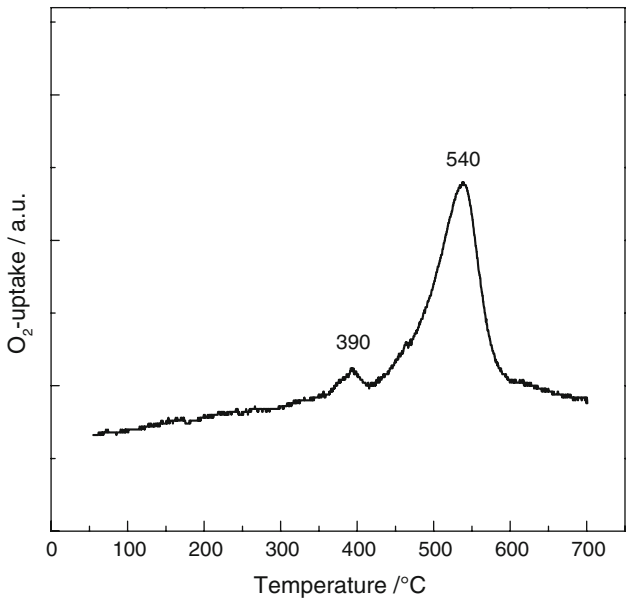

Fig. 3 TPO profile of as-prepared Mo_2C sample

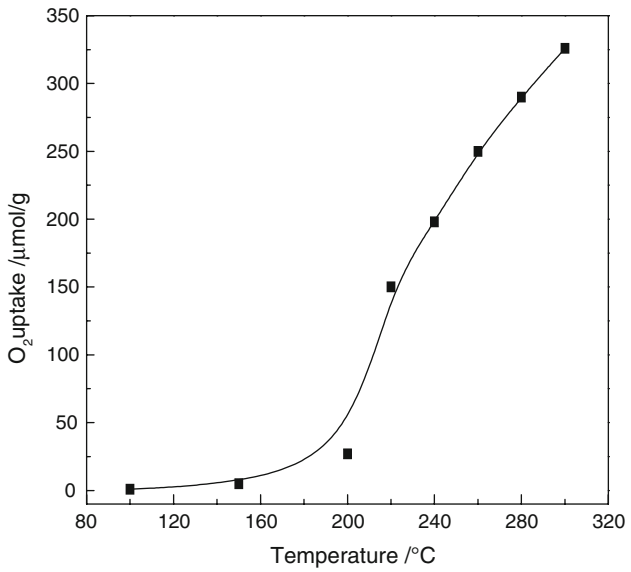

Fig. 4 O_2 uptake over Mo_2C sample as related to temperature

directly at 750 °C, the diffraction peaks of the resulted sample looked exactly the same as those of fresh one (Fig. 1). When the Mo_2C sample was heated at 850 °C, Mo_2C phase and a new set of X-ray peaks assigned to Mo phase were observed. On further heating in He at a higher temperature of 950 °C, the peaks of Mo_2C phase were diminished but those of Mo phase increased simultaneously. This was a clear indication that, Mo_2C was unstable at higher temperature above 750 °C in an inert atmosphere, and underwent slow decomposition to Mo metal with increasing temperature. Subsequently, the as-prepared Mo_2C sample was submitted to TPO experiment to investigate its structural stability in an oxidation environment. Figure 3 shows the TPO profile showing O_2 consumption with increasing temperature up to 700 °C. The amount of O_2 consumption increased with increasing temperature, and there were two O_2 consumption peaks at 390 and 540 °C, respectively. The former was weak whereas the latter was strong. According to the report of Liang et al. [24], Mo_2C surface is usually contaminated by polymeric carbon from the pyrolysis of CH_4 in temperature-programmed reduction procedure. Thus, it was reasonable to deduce that the O_2 consumption peak at low-temperature (390 °C) was due to the oxidation of surface carbon on Mo_2C sample, and that at a high temperature of 540 °C was due to the complete oxidation of Mo_2C bulk. Unfortunately, the TPO profile over Mo_2C can not provide sufficient detail about the start temperature for the bulk oxidation of the sample. For this reason, further O_2-uptake experiments were performed over Mo_2C sample. From Fig. 4, one can see that below 200 °C, the amount of O_2 adsorbed on the Mo_2C sample was very little. While the curve of oxygen uptake drastically increased above 200 °C probably due to progressive oxidation of carbon species. It was not possible to be confirmative whether the steep slope in O_2-uptake profile was due to oxidation of surface carbon or lattice carbon. We heated the as-prepared Mo_2C sample at 220 °C in air for 6 h. Subsequent XRD analysis (Fig. 5) of this sample yielded a two-phase mixture of Mo_2C and MoO_3, with the signals of the former much more intense than those of the latter. The result indicated that bulk oxidation of Mo_2C occurred at 220 °C in an oxidation environment. Based on the results of O_2-uptake and XRD

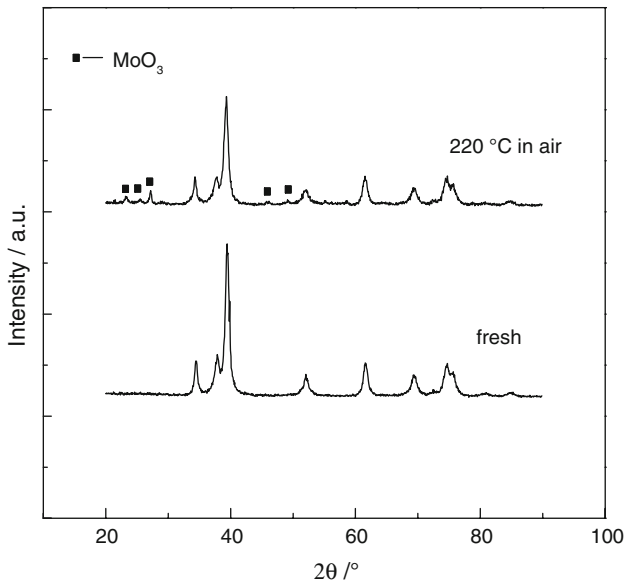

Fig. 5 XRD patterns of the Mo_2C sample during the heating treatment in air at 200 °C. The pattern of fresh Mo_2C is also shown for comparison

measurements as shown in Figs. 4 and 5, it was confirmed that the bulk Mo_2C suffered from oxidation above 200 °C.

3.2 Catalytic Activity on Temperature and Composition Dependence

Table 1 shows the temperature dependence of NO and CO conversion in 1:1 NO:CO reaction over Mo_2C catalyst. It can be seen that the Mo_2C catalyst showed low activity for conversion of NO to N_2 below 400 °C, but a high NO conversion to N_2 (about 95%) was achieved at or above 400 °C. The conversion of CO over Mo_2C was an activated process and was temperature dependent. One can see that CO conversion increased with increasing temperature, reaching 58% at 400 °C and declined to 52 and 45% at 500 and 600 °C, respectively. It was worthy to note that the conversion of NO was higher than that of CO at any temperature, except at 200 °C in which NO dissociation and reduction will not proceed (Table 1). The reaction we were expecting for the NO reduction with CO was stoichiometrically represented as:

$$2NO + 2CO = N_2 + 2CO_2 \quad (1)$$

However, based on the results of TPO and O_2-uptake (Figs. 3 and 4), it was deduced that the following oxidation of lattice carbon occurred:

$$C_{lattice} + xO_{ad} = CO_x (x = 1, 2) \quad (2)$$

O_{ad} will be produced by NO dissociation.

$$NO_{ad} = N_{ad} + O_{ad} \quad (3)$$

Therefore, the conversion of NO to N_2 was higher than that of CO because of the production of N_2 and CO_x ($x = 1, 2$) during the reaction between oxygen (generated from NO dissociation) and Mo_2C catalyst. The fact that there was a competition between NO reduction by CO and Mo_2C oxidation by oxygen species in the system. It was hence clear that the addition of CO concentration in NO/CO reaction was beneficial for avoiding bulk oxidation of Mo_2C catalyst.

Figure 6 shows the effect of feed composition on catalytic activity of Mo_2C catalyst in NO/CO reactions. It can be observed that the Mo_2C catalyst showed a stable activity of ca. 94% in a gas stream of 0.1%CO/0.1%NO/He at 400 °C, but deactivated rapidly after 12 h of on-stream reaction: NO conversion to N_2 decreased from ca. 94% to ca. 55% within a period of 20 h. With the addition of CO in the feed, the Mo_2C catalyst showed a stable activity of ca. 96% through out the test period of 20 h, no matter whether

Table 1 The temperature dependence of NO and CO conversion in 1:1 NO:CO reaction over Mo_2C catalyst

Temperature (°C)	Reaction time (h)	NO conversion to N_2 (%)	CO conversion (%)
200	5	0	0
300	5	24	12
400	10	94	58
500	10	95	52
600	10	95	45

Reaction conditions: NO = 1,000 ppm, CO = 1,000 ppm, gas flow rate = 20 cm^3 min^{-1}, W/F = 1.2 $gscm^{-3}$

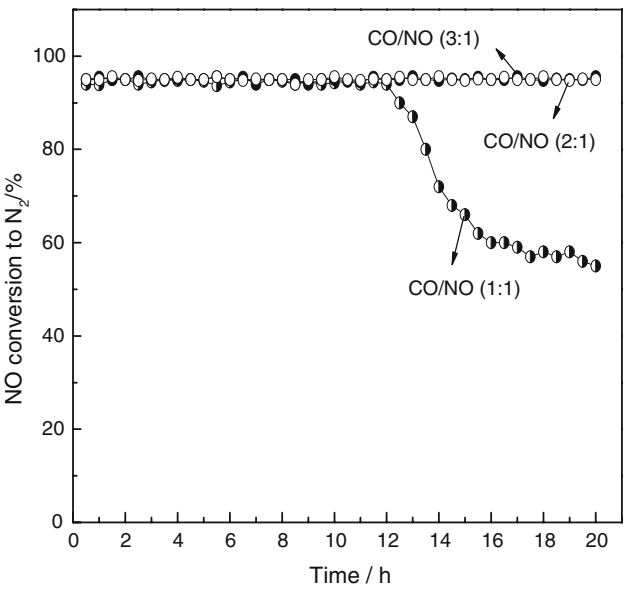

Fig. 6 The effect of feed composition on catalytic activity of Mo_2C catalyst in NO/CO reactions. Reaction conditions: CO = 1,000–3,000 ppm, NO = 1,000 ppm, gas flow rate = 20 cm^3 min^{-1}, W/F = 1.2 $gscm^{-3}$

Table 2 The effect of feed composition on catalytic activity of Mo_2C catalyst in NO/CO reactions

CO:NO ratio	NO conversion to N_2 (%)	CO conversion (%)	NO reduction degree (%)
1:1	94	57	57
2:1	96	43	86
3:1	96	32	96

Reaction conditions: NO = 1,000 ppm, CO = 1,000–3,000 ppm, gas flow rate = 20 cm^3 min^{-1}, W/F = 1.2 $gscm^{-3}$, reaction time = 10 h

it was in 0.2%CO/0.1%NO/He or 0.3%CO/0.1%NO/He. This indicated that the lifetime of Mo_2C catalyst can be prolonged when the feed gas was rich in CO. To better highlight the effect of NO:CO compositions on the catalytic activity of Mo_2C catalyst, the NO and CO conversion as well as NO reduction degree in the NO/CO reactions (1:1, 1:2 and 1:3 NO:CO compositions) at 400 °C are shown in Table 2. The nitrogen-containing reaction products was only N_2, without N_2O and other nitrogen oxides by analysis of MS and IRAS. Thus, the contributions of N_2 can be originated from the reaction Eqs. 1–3. As shown in Table 2, the conversion of NO to N_2 was closer in the three reactions. In addition, reasonable clear trends can be seen that, as the feed composition became gradually richer in CO, the consumption of CO increased and hence the NO reduction degree correspondingly increased. This was because, an addition of CO in feed gas could increase the CO concentration on the Mo_2C surface, which helped in the reduction of NO by CO (Eq. 1, in contrast, suppressed the reaction between oxygen (produced from NO dissociation) and Mo_2C catalyst (Eqs. 2, and 3). Notice that a complete equality of NO conversion and NO reduction degree seems to be achieved when the NO:CO ratio decreased to 1:3. The result indicated that the CO concentration in feed gas with 1:3 NO:CO ratio was sufficient to remove surface oxygen and establish a catalytic cycle over Mo_2C catalyst.

Subsequently, the used Mo_2C catalysts (functioned in 0.1%CO/0.1%NO/He and 0.3%CO/0.1%NO/He, respectively, at 400 °C for 20 h) were characterized by XRD. As shown in Fig. 7, the diffraction peaks for the Mo_2C catalyst used in 0.1%CO/0.1%NO/He for 20 h were still strong in intensities, but there were weak peaks due to MoO_2. It was a clear indication that the bulk Mo_2C can be oxidized by oxygen produced from NO dissociation in 0.1%CO/0.1%NO/He reaction. In other words, in NO/CO reaction with 1:1 NO:CO ratio, oxygen from NO dissociation would inevitably incorporate into the bulk of Mo_2C catalyst at 400 °C and hence can not be removed completely by CO, as shown in Table 2. Notice that diffraction pattern for the Mo_2C catalyst used in 0.3%CO/0.1%NO/He for 20 h was

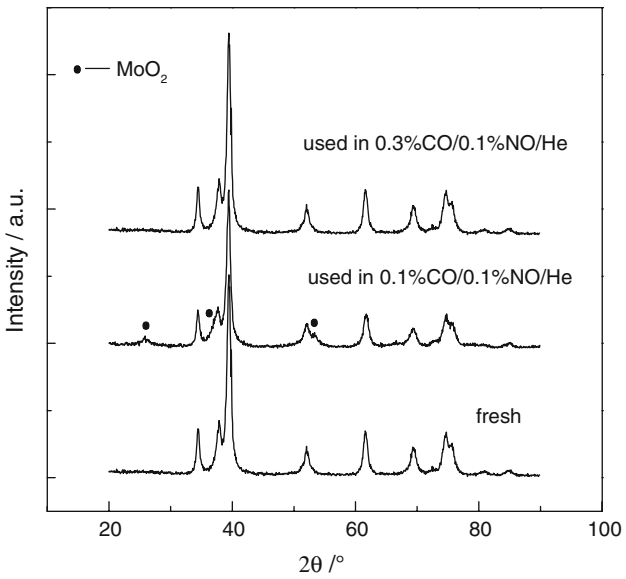

Fig. 7 XRD patterns of used Mo_2C samples as well as fresh sample for comparison

identical to that of the fresh sample. These results indicated that a NO/CO ratio of 1/3 was required to avoid bulk oxidation of Mo_2C catalyst in NO/CO reaction, which agreed well with the results that a catalytic cycle can be establish over Mo_2C catalyst in 0.3%CO/0.1%NO/He at 400 °C (Table 2).

3.3 Reaction Mechanism

Non-isothermal experiment, the so-called TPR experiment, was performed to examine surface reactivity of NO on Mo_2C catalyst. Figure 8a shows the variation of MS signal as a function of temperature during TPR. It can be seen that the degree of $m/e = 30$ (NO) adsorption and dissociation increased with temperature, and the production of $m/e = 44$ (N_2O or CO_2) and $m/e = 28$ (N_2 or CO) peaks occurred at 320 °C. At temperatures above the peak, complete NO conversion was coincident with the point at which the product of $m/e = 28$ (N_2 or CO) reached a higher plateau but that of $m/e = 44$ (N_2O or CO_2) reached the minimum concentration. With a further increase in temperature, the concentration of $m/e = 28$ (N_2 or CO) and $m/e = 44$ (N_2O or CO_2) increased and reached a maximum at 600 °C. It was worthy to note that the $m/e = 32$ (O_2) generated during NO dissociation was note detected in the whole temperature range. As shown in Fig. 8b, the concentration of N_2O, CO and CO_2 in the outflow gas are determined by IRAS. The N_2O formation was observed with a weak peak between 170 and 420 °C, coinciding with a weak formation peak of CO in this temperature range. At temperatures above 450 °C, the concentration of CO and CO_2 increased with increasing temperature and simultaneously reached the maximum at

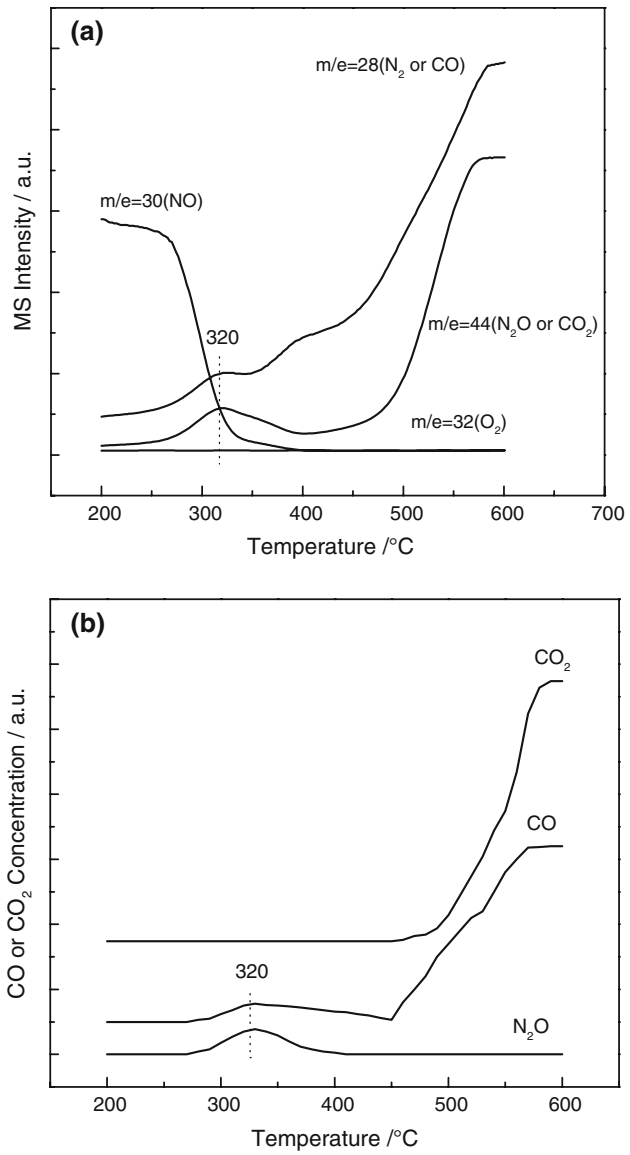

Fig. 8 TPR of Mo_2C catalyst followed by MS and IRAS

600 °C. Based on the result of MS-IRAS analysis, we deduced that N_2 and N_2O were formed during NO dissociation over Mo_2C surface at low temperature (below 320 °C). Coincidentally, CO was generated from the surface reaction between oxygen (originated from NO dissociation) and Mo_2C. In addition to a relatively high temperature, Mo_2C catalyst was more active toward NO dissociation and more selective toward the formation of N_2 (about 100%). The reaction between oxygen and Mo_2C surface was different from that at low temperature in terms of both CO and CO_2 formation, indicating that the oxygen species might have a strong oxidation capability for Mo_2C catalyst at high temperature.

From the results of Tables 1 and 2, it was clear that Mo_2C catalyst was active for NO reduction with CO, and that there was an enhancement in both activity and stability when there was a rise in CO concentration within the feed. However, from Fig. 8, it was found that there were not only NO dissociation reactions occurring on the Mo_2C surface, but also oxidation reaction occurring between oxygen generated from NO dissociation and Mo_2C. Therefore, in an attempt to understand the reaction mechanism of Mo_2C catalyst for NO reduction with CO, we differentiated the contributions of the following reactions to the conversion of NO to N_2.

3.3.1 NO Dissociation and Mo_2C Oxidation

It has been shown in Fig. 8 that NO was converted to N_2 in the absence of CO over Mo_2C catalyst, with detectable production CO_x ($x = 1, 2$) rather than O_2. Based on the results of RAIRS and TPD studies over β-Mo_2C [20] as well as surface reaction of $N^{15}O$ over C/Mo/W (111) and C/W (111) [21, 25], the surface reactions of NO over Mo_2C catalyst can be described as follows:

$$\mathrm{NO(g)} + * \leftrightharpoons \mathrm{NO}* \quad (4)$$

$$\mathrm{NO}* + * \leftrightharpoons \mathrm{N} * + \mathrm{O}* \quad (5)$$

$$2\mathrm{N} * \leftrightharpoons \mathrm{N_2} * + * \quad (6)$$

$$\mathrm{N_2} * \leftrightharpoons \mathrm{N_2(g)} + * \quad (7)$$

$$\mathrm{NO(g)} + \mathrm{NO} * \leftrightharpoons \mathrm{ON} * \mathrm{NO} \quad (8)$$

$$\mathrm{ON} * \mathrm{NO} + * \leftrightharpoons \mathrm{N_2O} * + \mathrm{O}* \quad (9)$$

$$\mathrm{N} * + \mathrm{NO} * \leftrightharpoons \mathrm{N_2O} * + * \quad (10)$$

$$\mathrm{N_2O} * \leftrightharpoons \mathrm{N_2O(g)} + * \quad (11)$$

$$x\mathrm{O} * + \mathrm{C_{lattice}} \rightarrow \mathrm{CO}_x * \ (x = 1, 2) \quad (12)$$

$$\mathrm{CO}_x * \leftrightharpoons \mathrm{CO}_x\mathrm{(g)} + * \ (x = 1, 2) \quad (13)$$

Oxygen produced during NO dissociation was partly released into the gas phase as N_2O (g); the rest was captured by Mo_2C catalyst. Heavy accumulation of surface oxygen resulted in gradual diffusion of oxygen into the carbide lattice and caused the ultimate oxidation of the bulk.

3.3.2 NO Reduction with CO

In the NO reduction reaction, the poisonous effect of oxygen toward Mo_2C can be eliminated by regulating the CO concentration in the feed; the process can be described as follows:

$$\mathrm{CO(g)} + * \leftrightharpoons \mathrm{CO}* \quad (14)$$

$$\mathrm{CO} * + \mathrm{O} * \leftrightharpoons \mathrm{CO_2}* \quad (15)$$

$$\mathrm{CO_2} * \leftrightharpoons \mathrm{CO_2(g)} + * \quad (16)$$

In NO reduction reaction, CO facilitated the removal of surface oxygen and hence one avoided the oxidation of

lattice carbon. According to the results of activity studies and XRD characterization (Table 2; Fig. 7), a minimum of 0.3% of CO in the 0.1%NO/He feed was required for establishing a catalytic cycle and avoiding bulk oxidation of Mo_2C catalyst.

4 Conclusions

Mo_2C catalyst was synthesized via CH_4/H_2-temperature-programmed reduction, and its structural properties were characterized by XRD, TPD, TPO and O_2-uptake techniques. In an inert atmosphere, the Mo_2C was unstable at higher temperature above 750 °C, and underwent slow decomposition to Mo metal with increasing temperature. Wherein an oxidation atmosphere, the start oxidation temperature of Mo_2C was above 200 °C and complete oxidation of its bulk occurred at 540 °C. In NO/CO reaction with 1:1 NO:CO ratio, the conversion of NO to N_2 was higher than that of CO at any temperature above 200 °C. Based on the results of TPO, O_2-uptake and TPR, we deduced that there was a competition between NO reduction by CO and Mo_2C oxidation by oxygen generated during NO dissociation. It was hence clear that an increase of CO concentration in NO/CO reaction was beneficial for avoiding bulk oxidation of Mo_2C catalyst. We found that surface oxygen from NO dissociation could be effectively removed by CO at 400 °C in 1:3 NO:CO reaction, and cycles of catalytic dissociation of NO can be achieved using Mo_2C as catalyst.

Acknowledgments The work was supported by the National Natural Science Foundation of China (No. 20573014) and by the Program for New Century Excellent Talents in University (NCET-07-0136).

References

1. Smeets PJ, Groothaert MH, van Teeffelen RM, Leeman H, Hensen EJM, Schoonheydt RA (2007) J Catal 245:358
2. Kustova MY, Rasmussen SB, Kustov AL, Christensen CH (2006) Appl Catal B 67:60
3. Wang C, Wang X, Xing N, Yu Q, Wang Y (2008) Appl Catal A 334:137
4. Wang X, Sigmon SM, Spivey JJ, Henry Lamb H (2004) Catal Today 96:11
5. Li L, Zhang F, Guan N, Schreier E, Richter M (2008) Catal Commun 9:1827
6. Kotsifa A, Kondarides DI, Verykios XE (2008) Appl Catal B 80:260
7. Galvez ME, Boyano A, Lazaro MJ, Moliner R (2008) Chem Eng J 144:10
8. Iwakuni H, Shinmyou Y, Yano H, Matsumoto H, Ishihara T (2007) Appl Catal B 74:299
9. Zhang Z, Geng H, Zheng L, Du B (2005) J Alloys Compd 392:317
10. Haneda M, Kintaichi Y, Nakamura I, Fujitani T, Hamada H (2002) Chem Commun p 2816
11. Naito S, Iwahashi M, Kawakami I, Miyao T (2002) Catal Today 73:355
12. Haneda M, Kintaichi Y, Nakamura I, Fujitani T, Hamada H (2003) J Catal 218:405
13. Patterson PM, Das TK, Davis BH (2003) Appl Catal A 251:449
14. Kojima R, Aika K (2001) Appl Catal A 219:141
15. Tominaga H, Nagai M (2007) Appl Catal A 328:35
16. Pritchard ML, Mclauley RL, Gallaher BN, Thomson WJ (2004) Appl Catal A 275:213
17. Li S, Lee JS, Hyeon T, Suslick KS (1999) Appl Catal A 184:1
18. Szymańska-Koalsa A, Lewandowski M, Sayag C, Djéga-Mariadassou G (2007) Catal Today 119:7
19. Lewandowski M, Szymańska-Koalsa A, Da Costa P, Sayag C (2007) Catal Today 119:31
20. Wang J, Castonguay M, Deng J, McBreen PH (1997) Surf Sci 374:197
21. Zhang M, Hwu HH, Buelow MT, Chen JG, Ballinger TH, Andersen PJ (2001) Catal Lett 77:29
22. Wang J, Ji S, Yang J, Zhu Q, Li S (2005) Catal Commun 6:389
23. Neylon MK, Choi S, Kwon H, Curry KE, Thompson LT (1999) Appl Catal A 183:253
24. Liang C, Ma W, Feng Z, Li C (2003) Carbon 41:1833
25. Zhang MH, Hwu HH, Buelow MT, Chen JG, Ballinger TH, Andersen PJ, Mullins DR (2003) Surf Sci 522:112